An Investigation into Turbine Blade Tip Leakage Flows at High Speeds

Z. Saleh, E. J. Avital, and T. Korakianitis

Abstract—The effect of the blade tip geometry of a high pressure gas turbine is studied experimentally and computationally for high speed leakage flows. For this purpose two simplified models are constructed, one models a flat tip of the blade and the second models a cavity tip of the blade. Experimental results are obtained from a transonic wind tunnel to show the static pressure distribution along the tip wall and provide flow visualization. RANS computations were carried to provide further insight into the mean flow behavior and to calculate the discharge coefficient which is a measure of the flow leaking over the tip. It is shown that in both geometries of tip the flow separates over the tip to form a separation bubble. The bubble is higher for the cavity tip while a complete shock wave system of oblique waves ending with a normal wave can be seen for the flat tip. The discharge coefficient for the flat tip shows less dependence on the pressure ratio over the blade tip than the cavity tip. However, the discharge coefficient for the cavity tip is lower than that of the flat tip, showing a better ability to reduce the leakage flow and thus increase the turbine efficiency.

Keywords—Gas turbine, blade tip leakage flow, transonic flow.

I. INTRODUCTION

THE design of a high pressure (HP) turbine blade tip has a considerable impact on the performance of the unshrouded turbine as blade-tip losses can contribute up to one third of the total stage losses. Recently there has been a significant amount of interest in the thermo-fluid dynamics of turbine blade tip flows. Experimental measurements and CFD predictions of blade-tip Nusselt numbers and tip leakage losses were carried out. In subsonic conditions, these studies mostly required matching the engine-scale Reynolds numbers. However, for transonic conditions such as when the blade-exit Mach numbers exceeds 0.8 (as commonly occurs in High Pressure turbines) the effects of compressibility become significant, particularly within the tip gap itself. Most of the studies into turbine tip flows have been carried out for low speed or subsonic turbine cascades as summarized in Ref. [1]. Far fewer studies have been performed at transonic or supersonic Mach numbers due to the complexity of the experimental testing and the flow computations. An old but rather genius approach to illustrate high speed compressible flow is to use a water table method while relying on the hydraulic analogy between compressible potential flow and free surface shallow water flow [2]. Such experiments showed that the formation of the vena-contracta at the entrance to the tip gap was able to accelerate the flow to supersonic conditions when the gap exit Mach number exceeded 0.8 [3]. Furthermore, the experimental and numerical tests of Chen et.al. [4] for a two dimensional tip gap in transonic flow showed that for an exit Mach number of 1.0, the peak Mach number in the gap was 1.4. They also found that when the tip flow speed was increased from subsonic to supersonic the separation bubble at the inlet to the gap reduced significantly in length. A more recent study has shown that the supersonic flow effects within a HP turbine-row can reduce the tip heat-load by up to 50% [5].

The aim of the project is to investigate the effect of two blade tip geometries on the flow leaking over the tip of a high pressure turbine blade. A reduction in the flow leakage can potentially lead to a significant improvement in the turbine thermodynamic efficiency and in its structural integrity due to the reduced exposure to high temperature. This kind of effort resides well with other current studies to increase gas turbine efficiency by blade profile redesign [6] and overall gas turbine optimization [7].

For the purpose of this study a combined approach of experiments and computations has been carried out on a flat tip and a cavity tip models. The experimental and computational procedures are reported next, followed by analysis of the results and conclusions.

II. EXPERIMENTAL PROCEDURE

The experimental work was carried out in the transonic wind tunnel of the high speed section of the Whitehead aeronautical laboratory, Queen Mary University of London, UK.

This is a close circuit wind tunnel which has a working section with cross sectional dimension of 135mm by 127mm. The following diagrams show the two dimensional tip model geometries which were tested.

Z. Saleh. is with the School of Engineering and Materials Science, Queen Mary university of London, Mile End Road, London, E1 4NS UK (e-mail:z.saleh@qmul.ac.uk).

E. J. Avital is with the School of Engineering and Materials Science, Queen Mary university of London, Mile End Road, London, E1 4NS, UK (e-mail:e.avital@qmul.ac.uk).

T. Korakianitis is with the Park College of Engineering, Aviation and Technology, St. Louis University, Missouri 63103, USA (e-mail: korakianitis@alum.mit.edu).

World Academy of Science, Engineering and Technology
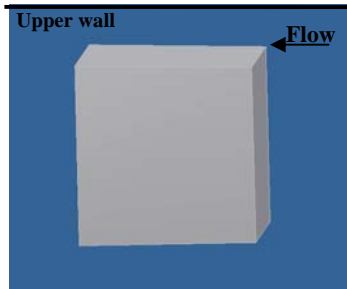International Journal of Aerospace and Mechanical Engineering
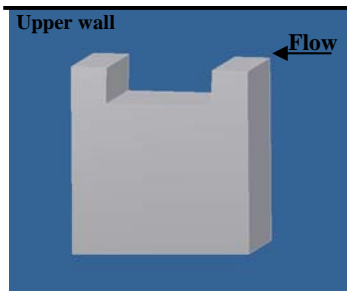Vol:7, No:1, 2013

Fig. 1 Flat Tip

Fig. 2 Cavity Tip

This tip model is similar in its approach to the model of Chen et al. [4]. The gap between the tip and the upper (casing) wall was about 15% of the wind tunnel work section height. This compares to the 10% gap of Chen et al.'s [4] for the flat tip. Pressure taps were mounted along the floor of the working section and on the surface of the tip model. Stagnation pressure was also measured far upstream of the model. Due to the small gap between the tip model and the upper wall of the work section strong vortical structures appeared behind the tip model, causing difficulties for the wind tunnel to operate. Thus a ramp in the form of a wedge was attached to the back side of the model to reduce the effect of such a wake on the ability of the wind tunnel to operate properly. Flow visualizations were carried out using the Schlieren method.

III. COMPUTATIONAL PROCEDURE

The Reynolds Averaged Navier-Stokes (RANS) equations approach has been used to compute the mean flow passing the blade tip model. The compressible Spalart-Allmaras model was employed along with the ANSYS CFD software.

The experimental conditions in the wind tunnel were reproduced using the computational domain shown in Fig. 3. The flow enters from the right side to the zone highlighted by the yellow background and exits on the left. Thus only the flow in front of the blade tip model and in the gap is considered. This saved the computational resources required to compute the strong wake behind the modeled blade tip. One should note that because the flow in the gap is expected to be high subsonic to supersonic thus the effect of this wake is expected to be negligible upstream if the right pressure ratio is prescribed between the far upstream condition and the exit of the gap as was done in this study.
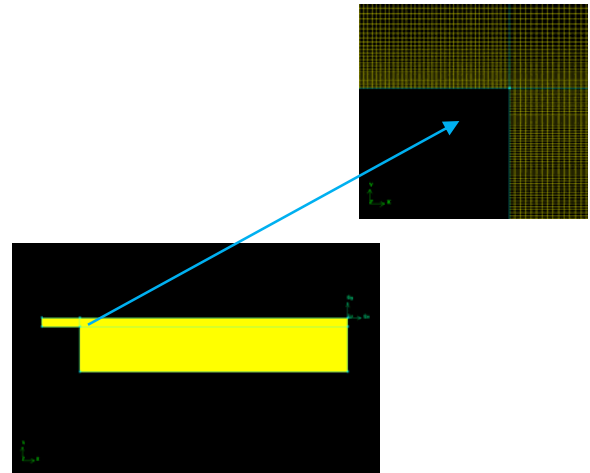

Fig. 3 The computational domain and mesh that was used for the flat tip model

A multi-block grid approach was used as illustrated in Fig. 3, leading to a high resolution in of about 250 grid points across the gap. This compares well with the recommendation of Chen et al. [4] for at least 100 grid points. The upper and the lower walls were taken as no-slip walls as well as the wall of the blade tip model to mimic the flow condition in the wind tunnel. All walls were assumed as adiabatic. A time implicit solver with a second-order spatial accuracy was used, where shock waves were captured using the MUSCL scheme. The y^+ value was checked after the computations to be less than 4 at the tip wall, showing an adequate resolution for RANS.

IV. RESULT

This section presents both the experimental and computational results and analysis for the flat and cavity tip models.

A. Flat Tip Results

Fig. 4 shows the distribution of the static pressure along the tip starting at the entrance to the gap at the pressure edge and ending on the suction edge which is the exit of the tip gap. The static pressure distributions are shown for three pressure ratios (PR) of the static pressure at the gap exit to the stagnation pressure far upstream of the gap. It is seen that as the PR reduces from the 0.65 to 0.57 the flow over tip changes from being subsonic to supersonic near the tip wall. This is marked by the sudden increase in the static pressure, indicating a shock wave. In all the cases there is a decrease in the pressure at the inlet and that is because the flow turns and accelerates at the inlet. Then the pressure level flattens for a short distance, indicating the presence of a separation bubble. At low PR values such as 0.57 the PR is sufficent to accelerate the tip flow to supersonic condition, causing the fluctuations in the pressure distribution due to a shockwave and its reflections from the upper wall. In general there is a fair agreement between the RANS and experimental results. The agreement is better for the high values of PR = 0.65, where a distrubtion typical for a subsonic flow is revealed. The

World Academy of Science, Engineering and Technology
International Journal of Aerospace and Mechanical Engineering
Vol:7, No:1, 2013

agreement is less fine after the shock wave occurance for the low level of PR. This is caused mainly by a disagreeement on the location of the shock wave.
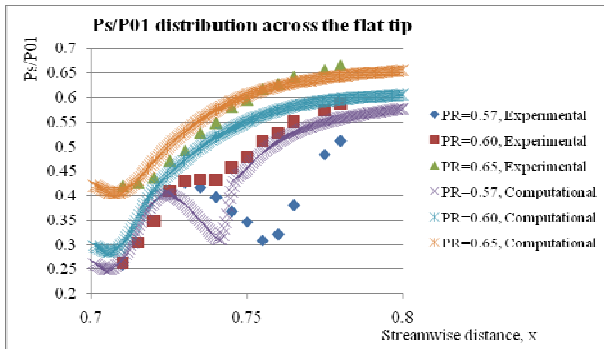

Fig. 4 Computational and experimental static pressure distributions along the flat tip for various pressure ratios (PR). PR is the ratio between the static pressure at the gap exit p_s and the stagnation pressure far upstream p_{01}

The computational Mach number contours and the experimental Schlieren flow visaulisation are shown in the fig. 5 and 6:
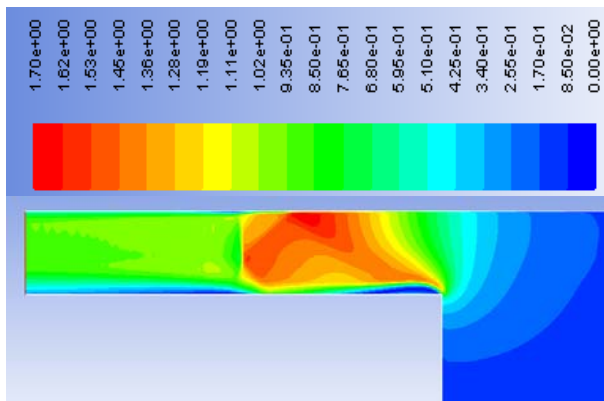

Fig. 5 Computational Mach number contours at PR=0.57 for the flat tip model

Fig. 6 Schlieren flow visualisation for PR=0.57 and flat tip model

It can be seen from both the computational and experimental results that as the flow enters the tip gap, it turns and accelerates as flow accelerates over a tip of an aerofoil. However as the leading edge of the tip is sharp in our case, the flow separates to form a separation bubble. This separation bubble at the leading edge forms a vena contracta through which the tip flow can further accelerate to a supersonic speed. Compression waves are formed on the aft portion of the separation bubble, merging together to form an oblique shockwave which reflects at the casing (upper) wall. This reflection is teminated by a normal shock wave. Both the computational and experimental results show the same flow behaviour and the qualitative agreement between Fig. 5 and 6 is good.

B. Cavity Tip Results

The computational pressure distribution along the cavity tip's wall is shown in Fig. 7 for three pressure ratios. The pressure is plotted only for the horizontal surfaces of the cavity tip. The cavity's front and aft rims are located at x= 0.70-0.72 and x=0.78-0.8, which can also be seen in Fig. 8. In both rims the pressure is close to flat. This indicates again flow separation as it happened near the flat tip entrance. As in that case, the pressure initially decreases due to the flow acceleration. However, the pressure increases towards the end of the forward rim until it levels off again showing further flow separation on the forward portion of the cavity floor. This pressure level increases again near the cavity's rear wall indicating stagnation zone near that wall and possible flow leakage through flapping of the shear layer. A small jump in the static pressure is seen at the rear edge of the cavity pointing to an increase in the pressure along the cavity's rear wall.
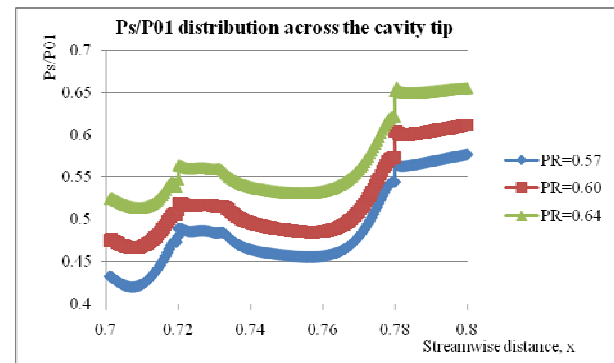

Fig. 7 Computational static pressure distributions of the cavity tip's horizontal walls

The computational Mach number contours and the experimental Schlieren flow visualisation results are illustrated in Fig. 8 and 9. Similar to the flat tip case, the flow enters the tip gap, turning and accelerating. The flow separates at the inlet and this separation acts as vena contracta to further accelerate the flow. In this case the PR value of 0.57 is suffiecent to accelerate the flow to a supersonic speed. Again as in the flat tip there are compression waves on the aft portion of the vena contracta, merging to form a shockwave, reflecting at the casing wall. However unlike the flat tip the reflected shock wave hits the cavity shear layer and thus the system of oblique shock waves followed by a normal shock wave seen in Fig. 6 is not seen in Fig. 9. Nevertheless, there is flow compression near the rear rim reducing the flow speed as

World Academy of Science, Engineering and Technology
International Journal of Aerospace and Mechanical Engineering
Vol:7, No:1, 2013

seen in both Figs. 8 & 9 and as was already indicated by the pressure distribution in Fig. 7.

Comparing the results for both the flat and cavity tip models, it is seen that the separation bubble in the case of the cavity does not reattach or in other words the width of the forward rim is not long enough to allow the separated flow to reattach. Also the height of this separation is higher than the one of the flat tip. These two differences have a favourate effect in reducing the tip leakage flow by reducing the effective tip gap height.
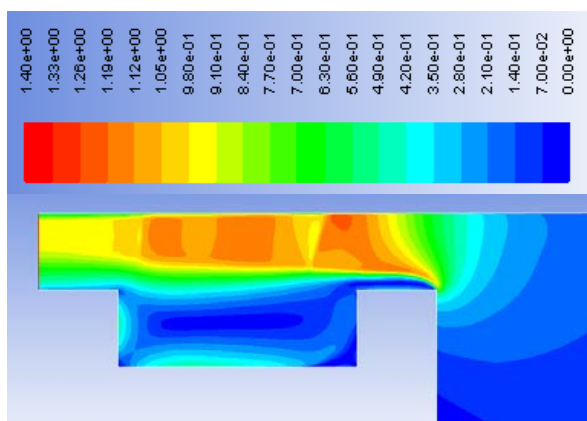

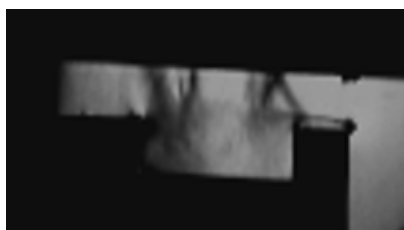Fig. 8 Computational Mach number countours for PR=0.57 and the cavity tip model

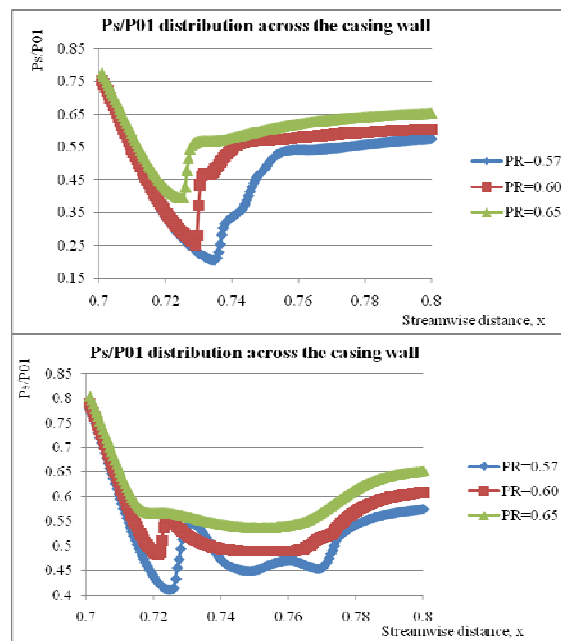Fig. 9 Schlieren flow visualisation, PR=0.57, cavity tip model

Fig. 10 Computational static pressure distrubtions along the upper (casing) wall for the flat tip (upper figure) and cavity tip (lower figure) models

The computational pressure distributions along the upper wall are shown in Fig. 10 for both the flat and cavity tips. All pressure distrbutions show a decline at the entrance to the gap due to the flow acceleration. Interestingly even the high PR value of 0.65 shows a jump in the wall pressure for the flat tip, indicating the occurance of compression waves near that wall. The further downstream pressure jumps for the lower PRs correspond to the system of oblique shock waves ending with an almost normal shock wave that is slightly tilted forward as seen in Fig. 6. The pressure distributions corresponding to the cavity model show much less prefound pressure jumps corresponding to the destruction of the shockwave system that was seen in Fig. 9.

C. Comparison between the Discharge Coefficient

The mass flow rate $\dot{m}_{act}$ and the discharge coefficient C_D were calculated using the below equations:

$$\dot{m}_{act} = \int_0^h \rho v_x dy \ , \qquad (1)$$

$$C_D = \dot{m}_{act} / \dot{m}_{isen} \ , \qquad (2)$$

ρ and v_x are the air density and streamwise velocity taken from the RANS computations and h is the gap height. $\dot{m}_{isen}$ is calculated assuming 1D isentropic flow [4]. The discharge coefficients of the two tip models are plotted in Fig. 11 for different pressure ratios.

World Academy of Science, Engineering and Technology
International Journal of Aerospace and Mechanical Engineering
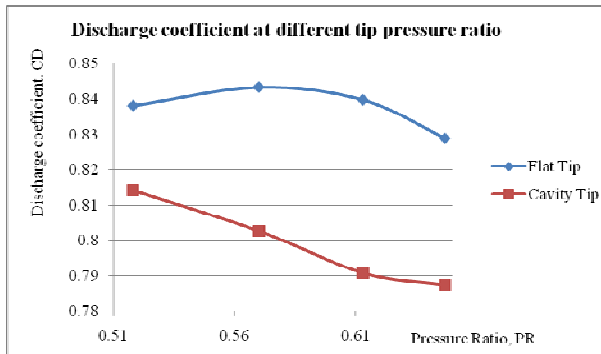Vol:7, No:1, 2013

Fig. 11 The discharge coefficient variation with the pressure ratio over the tip model

It is seen the discharge coefficient of the cavity tip is smaller than the flat tip at all PR values. As argued before, this is because the separation bubble does not reattach to the cavity's rim and its height is higher than the separation height on the flat tip. Hence the effective tip gap in the case of the cavity tip is smaller than in the case of the flat tip and therfore the leakage flow in the case of the cavity tip is smaller as compared to the flat tip. On the other hand the discharge coefficient in the case of the flat tip model is less sesnsitive to the values of the pressure ratios (PR), while reducing the PR values increases the level of the discharge cofficent for the cavity model.

V. Conclusion

A combined experimental-computational study was performed for two models of a high pressure turbine blade tip. The flat and cavity tips were modeled. Static pressure distributions along the tip models and flow visualizations were analyzed to show good qualitative agreement between the experimental study carried out in a transonic wind tunnel to RANS computations. It was found that in both cases, the flow separates at the inlet to the gap forming a vena contracta. In cases where the pressure ratio (PR) over the model was sufficient the vena-contracta created by the flow separation could accelerate the flow to supersonic speed leading to the formation of shockwaves. A complete system of two oblique shock waves followed by a normal shock wave was revealed for the flat tip. However this system was destroyed in the case of the cavity model. The effective tip gap in the case of the cavity tip was found to be smaller than that for the flat tip for the investigated pressure ratios. Hence the discharge coefficient was smaller for the cavity model.

Further work is carried out to investigate the effect of a flat tip and a cavity tip with round formed edges to model the effect of in-service erosion. This work will be communicated in the near future.

References

[1] Bunker RS, (2004), "Blade tip heat transfer and cooling techniques", VKI Lecture Series 2004-02.
[2] Bryant RAA (1960) "The Hydraulic Analogy for External Flow", Journal of the Aerospace Sciences, Vol. 27, No. 2 , pp. 148-149.
[3] Moore J, Elward KM, (1993) "Shock formation in over expanded tip leakage flow", ASME Journal of turbomachinary, vol.115, pp 392-399
[4] Chen G, Dawes WN, Hodson HP, (1993) "A numerical and experimental investigation of turbine tip gap flow" 29th Joint Propulsion Conference and Exhibit, AIAA 93-2253.
[5] Wheeler, A.P.S., Atkins N., and He, L. 2009 "Turbine blade tip heat transfer in low speed and high speed flows", GT 2009-59404, presented at the ASME Turbo Expo 2009, Orlando, Florida.
[6] Korakianitis T, Hamakhan I, Rezaienia MA, Wheeler APS, Avital EJ and Williams JJR (2012), Design of high-efficiency turbomachinery blades for energy conversion devices with the 3D prescribed surface curvature distribution blade design (CIRCLE) method. *Applied Energy*, Vol. 89 No. 1, pp. 215-227.
[7] Doulgeris G, Korakianitis T, Avital EJ, Pilidis P. and Laskaridis P., Effect of jet noise reduction on gas turbine engine efficiency *Proc IMechE Part G: J Aerospace Engineering,* 0954410012456925, first published on September 3, 2012.